# Collapse of an adsorbate island on substrate pillars

Koichi Takano and Yukio Saito
*Department of Physics, Keio University, 3-14-1 Hiyoshi, Kohoku-ku, Yokohama 223-8522, Japan*

Olivier Pierre-Louis
*Laboratoire de Physique de la Matière Condensée et Nanostructures, Université Lyon 1, 43 Boulevard du 11 novembre, 69622 Villeurbane, France*

(Received 29 March 2010; revised manuscript received 26 June 2010; published 10 August 2010)

We study an equilibrium shape of an adsorbate solid island on a substrate surface patterned with arrays of pillars. For a large island with a weak wettability to the substrate, an island sits on top surfaces of pillars, in a state called Cassie-Baxter (CB) state. In the opposite case of a small island with a strong wettability, the island collapses in the space between pillars, forming the so-called Wenzel (W) state. The collapse transition from CB to W state is studied in the phase space of the island volume and the wettability. Theory leads to collapse transition lines for an island with only (100) facets at zero temperature. They are in good agreement with the transitions observed in kinetic Monte Carlo simulations of an island with additional (110) and (111) facets at a finite temperature.

DOI: 10.1103/PhysRevB.82.075410 PACS number(s): 68.35.Rh, 81.16.Dn, 68.08.Bc

## I. INTRODUCTION

Wetting properties of liquid droplets are known to be strongly affected by patterning substrate surfaces.[1] When the substrate is patterned, for instance, with microscopic pillars, droplets may stay on top of the pillars with voids underneath. The state is called the Cassie-Baxter (CB) state,[2] and the equilibrium contact angle increases close to 180°. This superhydrophobicity affects flow properties of the droplet, and recently many studies are devoted on its large slippage length.[3–5] However, the liquid droplet can take another morphology, the Wenzel (W) state,[6] where the liquid fills the space between pillars. Then, the slippage length is largely reduced.

There are also many works on wetting and dewetting of solid adsorbate films on flat substrates.[7–11] When substrate surface is patterned, there is an additional effect on wetting properties of solid adsorbates such that the location and size of adsorption can be controlled.[12–16] On a substrate with nanopillars, one expects "supersolidphobicity," similar to the liquid droplets, but instead of the flow properties, improvement of the solid quality is expected.

In a heteroepitaxial crystal growth, there is, in general, a mismatch between lattice constants of adsorbate and substrate, and strain energy accumulated in an adsorbate film deteriorates its quality. In order to circumvent the strain effect, for instance, in the case of GaN growth on sapphire ($\alpha$-$Al_2O_3$), AlN or GaN buffer layers are provided at a low temperature, before thick GaN epilayers are grown at high temperatures.[17–20] The buffer layer actually consists of thin pillars, and the overgrown GaN crystal is free from strain and grows layer by layer with a flat surface to form a high-quality thick epilayer.

For optoelectronic purposes, GaN crystal is grown on Si substrate. Since there is a large lattice misfit in this system as well, various procedures are proposed. Among them is the growth of GaN on a Si substrate with arrays of pillars.[21] GaN islands start to grow mainly on the top surfaces of Si pillars, and they expand laterally leaving voids beneath.[21] There is another growth experiment on Si substrate with pores.[22,23] In this case, the adsorbed GaN forms islands leaving pores empty. The above examples indicate that adsorbate islands can grow with voids underneath, similar to the CB state in the liquid case. If the solid adsorbate fills in the gap between the substrate pillars as in the W state, the quality of the solid may be deteriorated. Therefore, it is important to understand the transition of solid islands between CB and W states on nanopillars.

The two states, CB and W, minimize the free energy at least locally. For liquid droplets, the transition is called the collapse transition and is studied theoretically and experimentally.[24–27] The collapse is observed when the droplet evaporates and its size becomes less than the lower limit.[24–26] Three scenarios are proposed for the collapse transition. For short pillars, enhancement of the local Laplace pressure pushes down the meniscus in the gap region between pillars and touch-down instability leads to the collapse transition.[25,27] For long pillars, disappearance of an energy barrier against depinning of the contact lines triggers the collapse.[27] In a recent experiment the above two scenarios cannot explain results, and then a new theory in terms of energy minimization is proposed.[26]

We study here the collapse transition of a solid adsorbate island on a substrate patterned with arrays of pillars. On the one hand, there are similarities between the solid and liquid cases. For example, we may expect similar trends of finite-size effects on the collapse transition. On the other hand, there are important differences. Indeed, in the case of solid islands, mass transport is dominated by surface diffusion, and the anisotropy of surface energies makes surfaces faceted at low temperatures. In Sec. II, we describe our lattice-gas model and procedures of kinetic Monte Carlo (KMC) simulations. Under certain simplifying assumptions in Sec. III, we obtain theoretically the minimum energy configuration of an equilibrium CB island on nanopillars, and analyze its stability through some collapsing paths. Our calculation corresponds to the contact-line depinning of a solid island on long pillars. Results are summarized in the collapse transi-

 

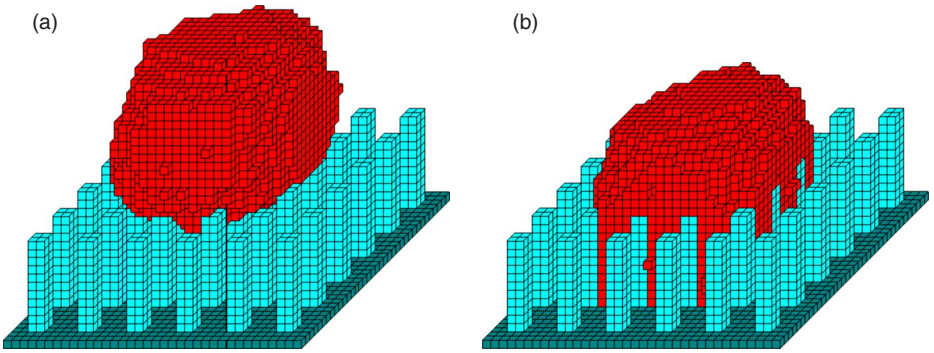


FIG. 1. (Color online) Two typical island morphologies on substrate pillars: (a) CB state and (b) W state. The reduced volume is the same $v=800$, but the wettability is different, (a) $\chi=0.390$ and (b) $\chi=0.405$. For visualization purpose, the flat base of the substrate has different color from the pillar parts.

tion diagram in the phase space of the island volume and the wettability. In Sec. IV, the phase diagram is compared with the results obtained by KMC simulations, and a good agreement is found. The result is summarized and the condition to grow solid islands without collapse is discussed in Sec. V.

## II. MODEL AND SIMULATION PROCEDURE

In order to study the equilibrium shape of a solid adsorbate island on a substrate with arrays of pillars, we extend our lattice-gas system used in the previous work.[16] On a simple cubic lattice a site is occupied by an adsorbed atom (or adatom), or by a substrate atom, or is empty. Substrate atoms are frozen and do not move. By starting from an adsorbate island on top of a patterned substrate, an island shape relaxes via the surface diffusion of adatoms along the island surface. An adatom is assumed to interact with the nearest-neighbor (NN) adatom with a bond energy $J_1$, and with the next-nearest-neighbor (NNN) adatom with a bond energy $J_2$. Their ratio $\zeta=J_2/J_1$ controls the equilibrium shape of an adsorbate solid. When $\zeta=0$, the equilibrium shape is cubic with (100) facets only. When $\zeta>0$, (110) and (111) facets appear in addition. At the zero temperature, facets are flat and their surface energy densities are

$$\epsilon_{1ij}=\frac{J_1}{2a^2}\sqrt{1+i^2+j^2}[1+(4-i-j)\zeta] \tag{1}$$

with $i,j=0$ or 1.

An adatom is assumed to interact with substrate atoms up to the second neighbors with bond energies $J_{s1}$ and $J_{s2}$. Their ratio is rather arbitrarily set equal to the one between two adatoms; $J_{s2}/J_{s1}=J_2/J_1=\zeta$. The ratio of adatom-substrate to adatom-adatom interactions

$$\chi=\frac{J_{s1}}{J_1} \tag{2}$$

defines the wettability of the adsorbate on the flat substrate. For example, in the case of large $\chi\geq 1$, the adsorbate completely wets the flat substrate. On the other hand, for $\chi\leq 0$, a flat substrate is completely dry. Between the two limits for $0<\chi<1$, partial wetting occurs. Wetting property changes if the substrate surface is no more flat but is modified with some patterns. Here we consider a substrate with a periodic arrangement of pillars. Each pillar has a square cross section with a width $\ell_p$ and a height $h_p$, and pillars are arranged in square arrays with a periodicity $\ell_x$. The ratio

$$\alpha=\frac{\ell_x}{\ell_p} \tag{3}$$

represents the relative periodicity. The substrate is completely frozen such that its shape does not change. The simulation box is periodic in $x$ and $y$ directions with a size $L_x \times L_x$. The box height $L_z$ is chosen high enough to accommodate the highest solid island.

In order to obtain equilibrium or metastable shape of an adsorbate island at a fixed volume $V$, we relax the island via surface diffusion by means of KMC simulations.[16] An adatom on the island surface is able to jump to one of its empty NN sites. When the adatom has $n_i$ numbers of neighbors of type $i=1,2,s_1,s_2$ prior to the jump, the transition probability is given as $\nu=\nu_0 \exp[-\Sigma_i n_i J_i/k_B T]$ with $\nu_0$ being an attempt frequency and $T$ the temperature. We set a temperature at $k_B T/J_1=0.5$ which is high enough to promote shape relaxation by surface diffusion of adatoms, but low enough to keep a faceted island shape. In order to keep the adatom on the surface of the island, we allow jumps to those empty sites that are connected to the island at least with one NN or NNN bond.

For an initial configuration of a simulation, we provide an adsorbate island with a rectangular parallelepiped shape which is close to a cubic form. After a KMC simulation, an adsorbate island ends up to one of the two typical morphologies, shown in Fig. 1. A CB state in Fig. 1(a) and a W state in Fig. 1(b). CB state is stable at small wettability $\chi$, but as $\chi$ increases the CB island collapses to W state.

## III. THEORETICAL ANALYSIS: $\zeta=T=0$

To allow an analytical study of the collapse transition, the model is further simplified in this section. We first assume that the NNN interaction is absent; $\zeta=0$. Then, the island is covered with only (001) facets. In addition, the temperature is set at absolute zero, $T=0$, so the energy minimization determines the equilibrium shape of an island. These two simplifications allow us to calculate analytically the equilibrium CB configuration and to study its stability against collapse transition. For an island extending over several pillars in the CB state, three typical conformations are found possible according to the island volume: (i) the inner, (ii) the pinned, and (iii) the outer states, as shown in Fig. 2. Stability analysis is undertaken for each state.

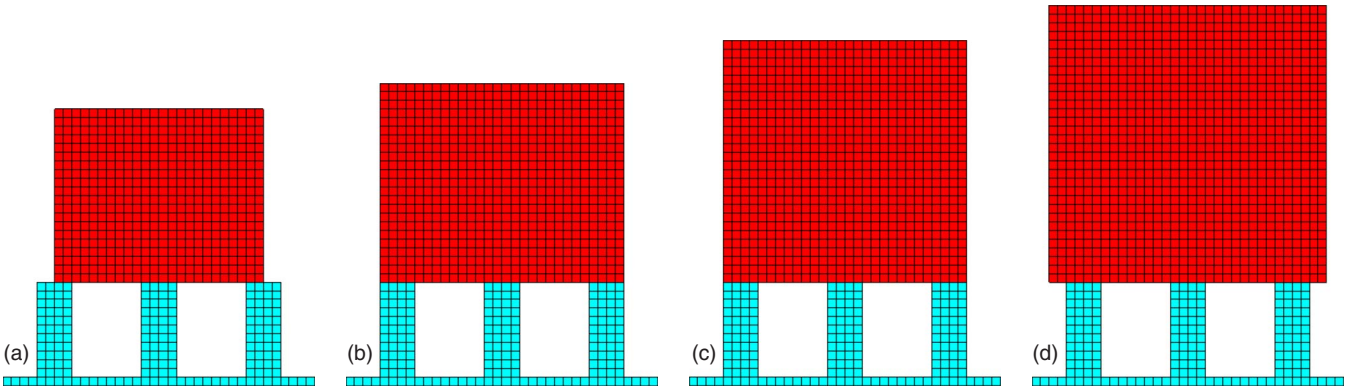


FIG. 2. (Color online) Side views of a CB island as it grows. (a) Inner state, (b) inner-to-pinned state, (c) pinned-to-outer state, and (d) outer state.

### A. Inner state

When an adsorbate solid is extending on top of $n \times n$ pillars of substrate, but its side edges remain inside the outermost pillars, as shown in Fig. 2(a), the state is denoted as "inner state." This CB inner state starts to collapse by wetting sidewalls of substrate pillars, as shown in a side view of Fig. 3(a). An island with a width $\ell$, a height $h$, and a wetting length $h^*$, has the volume $V=h\ell^2+h^*(n-1)(\ell_x-\ell_p)\{2\ell-(n-1)(\ell_x-\ell_p)\}$ and the surface energy

$$\frac{E}{\epsilon} = 2\ell^2 + 4\ell h - 2\chi\{\ell - (n-1)(\ell_x - \ell_p)\}^2 + 4(n-1)h^* \times [(\ell_x - \ell_p) + (1-2\chi)\{\ell - (n-1)(\ell_x - \ell_p)\}], \quad (4)$$

where $\epsilon=\epsilon_{100}$ for short. Since the island should not stick out from the outermost pillars, the width $\ell$ should remain in the range

$$(n-1)\ell_x - \ell_p \le \ell \le (n-1)\ell_x + \ell_p. \quad (5)$$

The equilibrium shape of an island in the CB state is determined by minimizing $E$ with respect to $\ell$ at a fixed volume $V$ and at $h^*=0$, and the lateral width $\ell$ is found to obey

$$(1-\chi)\ell^3 + (n-1)\chi(\ell_x - \ell_p)\ell^2 = V \quad (6)$$

with the height $h=V/\ell^2$. For $n=1$ the condition Eq. (6) reduces to the Wulff-Kaischew theorem[28,29] of an equilibrium island shape on a flat surface. It is easy to show that with a finite wettability $\chi$ the equilibrium shape of an island in an inner state is flatter than a cubic shape for arbitrary $n$; $\ell > h$.

The stability of the CB state against wetting is analyzed by studying $h^*$ dependence of an excess energy $\Delta E=E(h^*)-E_{\mathrm{CB}}(h^*=0)$ at a fixed volume $V$. Here $E(h^*)$ is the minimum energy obtained by varying $\ell$ for a given wetting length $h^*$ with $h$ being determined by the volume conservation. Resulting excess energy $\Delta E$ is shown in Fig. 4 as a function of $h^*$. For a large island with a volume $v=750$, there is an energy barrier and the island in the CB state with $h^*=0$ is metastable; finite perturbation is necessary for the island to collapse. For a small island ($v=720$) the energy barrier disappears, and the island is unstable against collapse. The collapse transition takes place at a critical volume $V_0$ when the slope $dE/dh^*$ at $h^*=0$ vanishes. It is obtained to be

$$V_0 = \{1 + (n-2)\chi - 2\chi^2(n-1)\}\left(\frac{\alpha - 1}{1-2\chi}\right)^3 \ell_p^3. \quad (7)$$

For $\alpha=3.0$ and $n=4$, the critical volume $V_0$ is represented as a function of wettability $\chi$ in the inner-state region in Fig. 5. For a given volume, the CB state becomes unstable when the wettability becomes strong. For a fixed wettability, the CB state becomes stable if the island volume increases. Dashed lines indicate the volume restriction for inner state derived from the restriction Eq. (5). Outside of these lines, other states are relevant.

### B. Outer state

As the island volume increases, it spills out from the outermost pillars, as shown in Fig. 2(d). This state is denoted as an "outer state." When this outer state undergoes a collapse transition, adatoms wet sidewalls of pillars within the $n\ell_x \times n\ell_x$ region, as shown in Fig. 3(b). This mode of deformation turns out to be the most unstable. Wetting the outside wall of the outermost pillars is energetically unfavorable for $\chi<0.5$. Partial collapse by wetting a smaller region of $m \times m$ pillars with $m<n$ is also found energetically unfavorable.

In the configuration of Fig. 3(b), the island has a volume $V=h\ell^2+h^*(n-1)(\ell_x-\ell_p)\{(n-1)\ell_x+(n+1)\ell_p\}$ with the surface energy

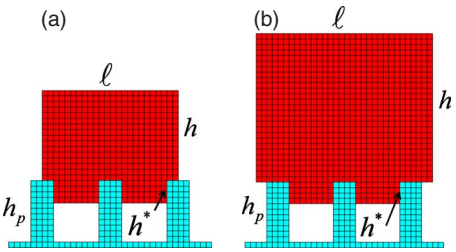


FIG. 3. (Color online) Side views of collapsing processes for (a) the inner state and (b) the outer state.

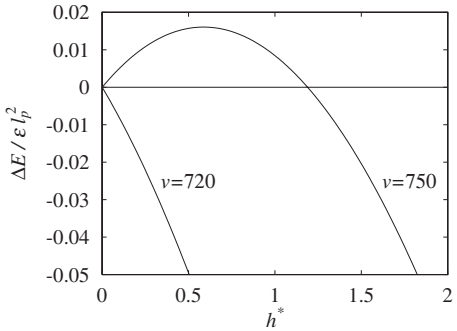


FIG. 4. Island excess energy $\Delta E = E - E_{CB}$ from a CB state as a function of a wetting length of a pillar sidewall $h^*$ at a wettability $\chi = 0.395$. A large island with a volume $v = V/\ell_p^3 = 750$ has an energy barrier, whereas a small island with a volume $v = 720$ has none. The critical volume is calculated as $v_0 = V_0/\ell_p^3 = 738$.

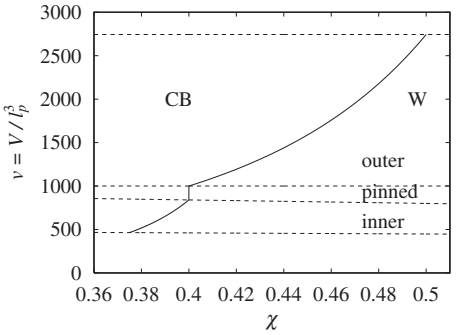


FIG. 5. The CB-W collapse transition line in the phase space of the reduced volume $v = V/\ell_p^3$ and the wettability $\chi$ for $\alpha = 3.0$ and $n = 4$. Dashed lines separate regions of inner, pinned, and outer states.

$$\frac{E}{\epsilon} = 2\ell^2 + 4\ell h - 2\chi n^2 \ell_p^2 + 4(n-1)h^*\{\ell_x - \ell_p + (1-2\chi)n\ell_p\}. \tag{8}$$

From the restriction that the island extends beyond the outermost pillars but does not reach the next pillars, the width $\ell$ is confined in a region

$$(n-1)\ell_x + \ell_p \leq \ell \leq (n+1)\ell_x - \ell_p. \tag{9}$$

When $h^* = 0$, the minimum energy configuration is found to be a cube ($\ell^3 = V$) independent of the wettability parameter $\chi$. Indeed, as long as the number $n^2$ of pillars in contact with the island is fixed, the contact with the pillars only gives a constant energy contribution, independent of the island morphology. As a consequence, the equilibrium shape is identical to that of a free standing island.

The study of the collapse transition follows the same lines as in the case of the inner state. The instability occurs when the slope $\partial E/\partial h^*$ vanishes at $h^* = 0$. A critical volume obtained

$$V_0 = \left[ (\alpha - 1)\frac{(n-1)\alpha + (n+1)}{\alpha - 1 + n(1-2\chi)} \right]^3 \ell_p^3 \tag{10}$$

is shown in the outer-state region in Fig. 5.

The two transition curves of the inner and outer states, however, are disconnected. Between the two regimes of inner and outer states, there is a third state for CB state: a pinned state, shown in Figs. 2(b) and 2(c).

### C. Pinned state

Let us consider the growth process of an adsorbate solid island in the CB state on $n \times n$ pillars, as shown in Fig. 2. A small island stays in an inner state [Fig. 2(a)], and the equilibrium shape is decided by Eq. (6), which is flat ($h < \ell$). As the volume increases, the lateral width $\ell$ of an island increases and eventually the island edges reach the exterior of the outermost pillars [Fig. 2(b)] at $\ell = (n-1)\ell_x + \ell_p$. Once the edge covers the whole top surface of the pillars, it is pinned for a while and the island grows only vertically. This state is defined as the "pinned state."[30] When a height $h$ reaches $\ell$, the island becomes cube as in Fig. 2(c), and edges are depinned for further growth. In an outer state the island keeps a cubic shape, Fig. 2(d). Since the island width $\ell$ is kept constant in the pinned state, the energy of the CB state with $h^* = 0$ is proportional to the volume as $E_{pin}(V)/\epsilon = 2(\ell^2 - \chi n^2 \ell_p^2) + 4V/\ell$. Since the pinned state has a high energy, it is possible only in the volume region where no other states exist, as shown in Fig. 5.

The collapse of pinned CB state is again assigned at the place when the slope $\partial E/\partial h^*$ vanishes at $h^* = 0$. It is found to take place at a constant $\chi$;

$$\chi = \frac{(n-2)\alpha + 2}{2\{(n-1)\alpha + 1\}}, \tag{11}$$

independent of the volume. The collapse transition line of an island thus turns out to be continuous over various states, as shown in Fig. 5, as long as the underlying number of pillars $n \times n$ is fixed.

### D. Transition between different *n* states

So far, our analysis of collapse transition is restricted in a certain volume range, because the number $n^2$ of pillars underneath is fixed. But as the solid volume increases, numbers involved should increase as well. We consider now the transition between different $n$ states.

By comparing energies of various CB states with different $n$'s in different states, we search the minimum energy configuration and find that the $v$-$\chi$ phase space is divided into zones of different $n$'s, as shown by dashed lines in Fig. 6. The $n = 4$ CB state, for instance, has the minimum energy in the $n = 4$ zone, but it extends in $n = 3$ and 5 zones as a metastable state.

In Fig. 6, the collapse transition lines are shown too by straight curves. The parts extending in the neighboring metastable zones are drawn by dotted lines. For example, let us consider collapse transitions in the $n = 4$ zone. Here, the CB island on $4 \times 4$ pillars has the minimum energy, and it collapses to the W state when $\chi$ is larger than the value of continuous collapse line. However, to the left of the dotted collapse line which is extending from the $n = 3$ zone, the metastable CB island on $3 \times 3$ pillars is still stable against

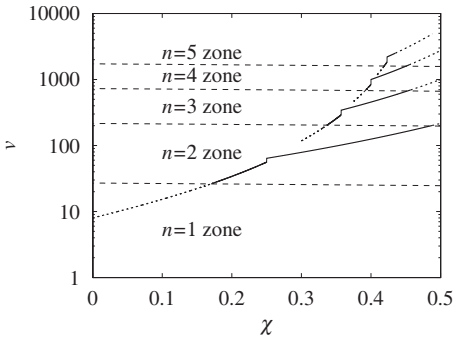


FIG. 6. The phase space $v$-$\chi$ is divided into zones where $n$ CB state is the most stable one for $n=1-5$. Lines indicate the collapse transition lines for various CB state.

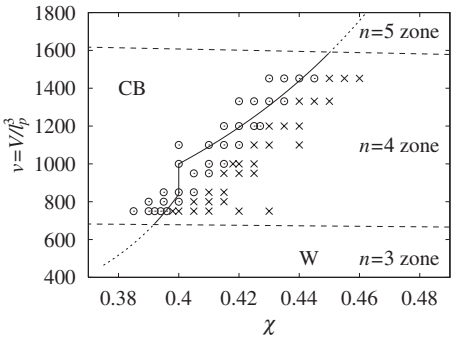


FIG. 7. Summary of KMC simulation results on collapse transition for $n=4$ and $\alpha=3$. Circles correspond to the stable CB states and crosses to the W states. The line corresponds to the theory on the collapse of a (100)-faceted island.

collapse. Therefore, the island started on $3\times3$ pillars may not collapse, if it grows fast enough so as to pass through the $n=4$ collapsing region staying in $n=3$ state until it reaches the large volume where $n=4$ CB state is stable. On the contrary, if the island touches to outer pillars and increases $n$ in the 3–4 coexistence region, then it collapses to the W state. This type of time-dependent phenomena can be studied only by KMC simulations.

## IV. SIMULATION OF ISLAND SHAPE: $\zeta=0.2$ AND $k_BT/J_1=0.5$

An adsorbate solid island relaxes its shape by surface diffusion at a finite temperature, that is set at $k_BT/J_1=0.5$. In order for adatoms turn around edges and corners of an island, the NNN bonds are required, since the NN bonds are broken there. In the following KMC simulations, we set a small attractive NNN interaction as $\zeta=J_2/J_1=0.2$. Substrate forms high square pillars of a width $\ell_p=2$ arranged in a square array with a periodicity $\ell_x=6$. The relative periodicity $\alpha=\ell_x/\ell_p$ is then 3.

### A. Collapse of a CB state with a fixed $n$

First, we study the collapse transition of a CB island on $n\times n$ pillars with parameter values corresponding to those in the $n$ zone. We describe results for the case with $n=4$. The collapse transition is monitored by the wetting length $h^*$, since it is equal to the pillar height, when the island collapses. For a fixed normalized volume of $v=V/\ell_p^3=800$, the collapse transition takes place between $\chi=0.400$ and $\chi=0.405$. The last configuration of a solid island in CB state is shown in Fig. 1(a) for $\chi=0.39$ and that in W state in Fig. 1(b) for $\chi=0.405$.

Simulation results with various combinations of island volume $v$ and wettability $\chi$ are summarized in a $v$-$\chi$ phase diagram in Fig. 7. For a large island or for a poor wettability, the CB state of an island sitting on pillars remains stable. The collapse transition takes place close to the theoretical curve, obtained in the previous section. In a closer look, one finds that for a given volume the CB state remains stable against the larger wettability $\chi$ than the theoretical value. Also there is no sharp transition among inner, pinned, and outer states, observed in theoretical analysis. These discrepancies may be due to the finite NNN interaction $J_2$, which allows the (110) and (111) facets; we observe that these facets penetrate into the gap among pillars and support CB island from collapsing.

### B. Collapse of a CB state associated with $n$ variation

In a certain region of $v$-$\chi$ phase space, multiple of CB states coexist, as shown in Fig. 6. One has the lowest energy, but the others can exist as metastable states.

For example, in the region of $n=4$ zone but close to the $n=3$ zone, as shown in Fig. 8, $n=3$ CB state is metastable, and we can prepare an initial island on $3\times3$ pillars. When an island is large with a volume $v=1050$ and the wettability is small as $\chi=0.40$, an island is in the stable region of $n=4$ CB state, as marked by the upper-left circle in Fig. 8. During the shape relaxation, the island changes numbers of pillars beneath it from (a) $3\times3$ to (b) $3\times4$ and finally to (c) $4\times4$, as shown in Fig. 9. The island relaxes to the most stable configuration with $n=4$.

If the volume is small as $v=729$ with the same wettability $\chi=0.40$, as shown by the lower circle in Fig. 8, the island started on $3\times3$ pillars remains on the same $3\times3$. Since it lies to the left of the collapse transition line for $n=3$, the island remains in the CB state without collapse, even though it is in the collapse region to the right of black collapse line of $n=4$. With the same volume $v=729$ but with very strong wettability as $\chi=0.47$ (the rightmost cross in Fig. 8), the $n=3$ island collapse quickly, since it lies to the right of the

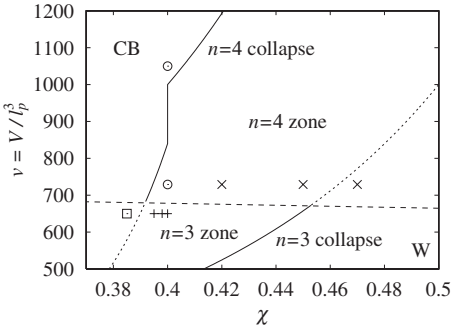


FIG. 8. Phase space close to $n=3$ and 4 zones.

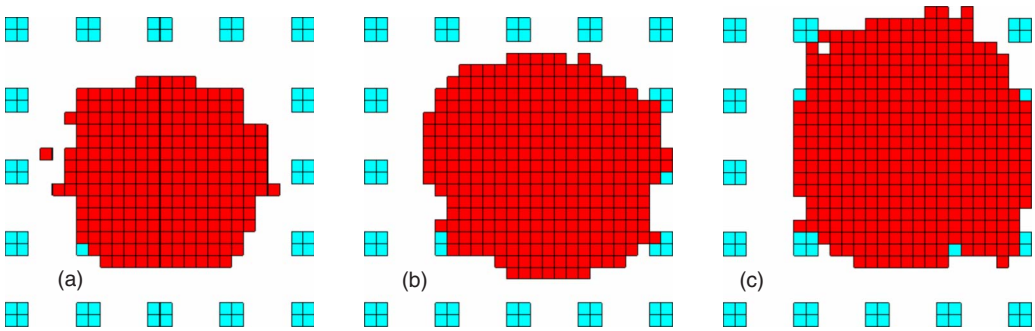


FIG. 9. (Color online) Variation of a number of pillars in touch of a base facet at a level of pillar top. (a) At the time $t\nu_0=2\times10^4$, base sits on $3\times3$ pillars, (b) at $t\nu_0=6\times10^4$, it is on $3\times4$ pillars, and eventually (c) at $t\nu_0=5\times10^5$, it is on $4\times4$ pillars. The island volume is $v=1050$ and the wettability is $\chi=0.40$.

collapse transition line for $n=3$. In the case of intermediate strength of wettability $\chi=0.42$ and 0.45, the number of pillars underneath changes and the island collapses. The initial CB island supported on $3\times3$ pillars is stable, since the parameter lies to the left of $n=3$ collapse transition line. However, to decrease the island energy, numbers of pillars beneath changes from $3\times3$ to $3\times4$ and eventually to $4\times4$, similar to the process shown in Fig. 9. Once the transition from $n=3$ to 4 states occurs, the collapse transition line for $n=4$ becomes relevant, and thus the island collapses.

Now we consider the opposite region; $n=3$ zone close to the $n=4$ zone, as shown in Fig. 8. The situation can be realized by evaporation. A large island is initially in the $n=4$ stable region and is in a CB state on $4\times4$ pillars. Then, by evaporation the island volume decreases into the $n=3$ region. How will the island behaves when the volume is reduced? Simulations are performed at a fixed reduced volume $v=650$, and the wettability parameter $\chi$ is varied. Initially the CB island is set on $4\times4$ pillars, but it is metastable.

For large $\chi\geq0.395$ marked by plus symbols in Fig. 8, the island collapse rapidly since it has no time to rearrange into $n=3$ configuration. Then, the $n=4$ collapse line comes into play and the island collapses to W state. With a small wettability as $\chi=0.385$, as shown by a square symbol in Fig. 8, the island is in the region where $n=4$ CB state is stable against collapse. Therefore, an island remains a while in the CB state. In the meanwhile, the number of pillars beneath the island changes from $4\times4$ to $3\times4$ and then to $3\times3$, in the reverse order shown in Fig. 9. The true ground state is achieved. Since the island stays in the stable region of $n=3$ CB state, it is more stable than the initial configuration. Thus, we find that the shape of an island depends on the history of its preparation.

## V. SUMMARY AND DISCUSSIONS

We have studied the collapse transition of an adsorbate island on a substrate patterned with arrays of pillars. An island can sit on top of the pillars, called a CB state, or fill the space between them, called a W state. The CB state collapses to the W state as the island volume decreases.

In a simplified model of an island with only (100) facets at zero temperature, the CB state is further classified into three categories; the inner, the pinned, and the outer states. In an outer state, an equilibrium shape is the same with a free-standing island, cubic. This means that the adsorbate island is completely free from the substrate, even though there is a finite wettability $\chi$. The pillars make the substrate surface supersolidphobic.

As the island volume increases, the number $n\times n$ of pillars in contact with the island increases. The phase space of the volume $V$ and the wettability $\chi$ are divided into zones of CB states with different $n$'s, and the zone $n$ is approximately centered about $V\approx(n\ell_x)^3$ for large $V$, where $\ell_x$ is the pillar periodicity. However, the CB state collapses when an energy barrier against depinning of a wetting front disappears. As a wettability $\chi$ increases to 1/2, the critical volume $V_0$ of collapse in the pinned state, for example, increases approximately as $V_0\approx[(\ell_x-\ell_p)/(1-2\chi)]^3$, where $\ell_p$ is the pillar width.

The collapse transition line obtained by KMC simulations lies quite close to the one obtained by the above simplified theoretical analysis, albeit the island in KMC simulations has additional two facets, (110) and (111), and relaxes at a finite temperature. Simulation also confirms that the $v$-$\chi$ phase space is divided into zones according to the number $n$ of pillars underlying the CB island. Each zone extends to the neighboring zones as a metastable state. Collapse transition is affected by the metastability, since it depends on the number $n$ of the underlying pillars.

We may now ask the condition that an adsorbate island nucleated on top of one pillar can grow *without collapse* under quasiequilibrium conditions. A possible pathway in the

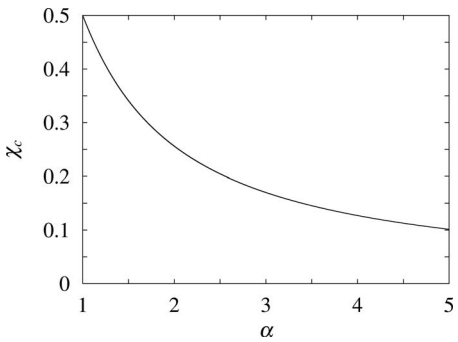


FIG. 10. Critical wettability $\chi_c$ versus relative periodicity $\alpha$.

$v$-$\chi$ phase diagram is the one where $v$ is increased at constant $\chi$. Such a quasistatic growth process is possible for $\chi < \chi_c$. Here $\chi_c$ corresponds to the value of $\chi$ for which the boundary between $n=1$ and $n=2$ zones crosses the collapse line for the inner state with $n=2$. The critical wettability $\chi_c$ depends on relative periodicity $\alpha$ only and is plotted in Fig. 10; smaller values of $\alpha$ are more favorable to island growth in the CB state without collapse.

In contrast, for the specific case of GaN/Si pillars growth,[21] the main motivation for growing islands in the CB state is to get rid of heteroepitaxial elastic stresses induced by the lattice mismatch. This is achieved when $\ell_p \ll \ell_x$, i.e., when $\alpha \gg 1$. Therefore, the two major constraints imposed by wettability and by elastic stresses seem to play in opposite directions, and a suitable choice of $\alpha$ must be a compromise between them.

Finally, the present equilibrium shape analysis is restricted to slow growth conditions, where the shape has an ample time to relax to the equilibrium one. In this regime, we have obtained a quite restrictive condition for the growth of islands in the CB state, which is essentially related to the collapse of small CB islands. Therefore, in order to keep an island on top of the pillars, it seems necessary to grow the island fast enough before the collapse takes place. Once the island grows large enough, further growth will be free of collapse. Hence, the study of the kinetics of CB island growth is a crucial direction for further investigations.

## ACKNOWLEDGMENTS

Y.S. acknowledges support by a Grant-in-Aid for Scientific Research (Grant No. 19540410) from the Japan Society for the Promotion of Science. O.P.L. acknowledges support by ANR-PNANO Grant "DéFiS."

[1] D. Quéré, Rep. Prog. Phys. **68**, 2495 (2005).
[2] A. B. D. Cassie and S. Baxter, Trans. Faraday Soc. **40**, 546 (1944).
[3] P. Joseph, C. Cottin-Bizonne, J.-M. Benoî, C. Ybert, C. Journet, P. Tabeling, and L. Bocquet, Phys. Rev. Lett. **97**, 156104 (2006).
[4] T. Biben and L. Joly, Phys. Rev. Lett. **100**, 186103 (2008).
[5] C. Lee, C.-H. Choi, and Chang-Jin Kim, Phys. Rev. Lett. **101**, 064501 (2008).
[6] R. N. Wenzel, Ind. Eng. Chem. **28**, 988 (1936).
[7] K. Thürmer, E. D. Williams, and J. E. Reutt-Robey, Phys. Rev. B **68**, 155423 (2003).
[8] E. Dornel, J.-C. Barbé, F. de Crécy, G. Lacolle, and J. Eymery, Phys. Rev. B **73**, 115427 (2006).
[9] O. Pierre-Louis, A. Chame, and Y. Saito, Phys. Rev. Lett. **99**, 136101 (2007).
[10] M. Khenner, Phys. Rev. B **77**, 165414 (2008).
[11] O. Pierre-Louis, A. Chame, and Y. Saito, Phys. Rev. Lett. **103**, 195501 (2009).
[12] I. Goldfarb, Nanotechnology **18**, 335304 (2007).
[13] A. Pascale, I. Berbezier, A. Ronda, and P. C. Kelires, Phys. Rev. B **77**, 075311 (2008).
[14] G. Katsaros, J. Tersoff, M. Stoffel, A. Rastelli, P. Acosta-Diaz, G. S. Kar, O. G. Schmidt, and K. Kern, Phys. Rev. Lett. **101**, 096103 (2008).
[15] T. U. Schülli, G. Vastola, M.-I. Richard, A. Malachias, G. Renaud, F. Uhlík, F. Montalenti, G. Chen, L. Miglio, F. Schäffler, and G. Bauer, Phys. Rev. Lett. **102**, 025502 (2009).
[16] O. Pierre-Louis and Y. Saito, EPL **86**, 46004 (2009).
[17] H. Amano, N. Sawaki, and I. Akasaki, Appl. Phys. Lett. **48**, 353 (1986).
[18] I. Akasaki, H. Amano, Y. Koide, K. Hiramatsu, and N. Sawaki, J. Cryst. Growth **98**, 209 (1989).
[19] K. Hiramatsu, S. Itoh, H. Amano, I. Akasaki, N. Kuwano, T. Shiraishi, and K. Oki, J. Cryst. Growth **115**, 628 (1991).
[20] S. Nakamura, Jpn. J. Appl. Phys., Part 2 **30**, L1705 (1991).
[21] S. D. Hersee, X. Y. Sun, X. Wang, and M. N. Fairchild, J. Appl. Phys. **97**, 124308 (2005).
[22] L. Macht, P. R. Hageman, S. Haffouz, and P. K. Larsen, Appl. Phys. Lett. **87**, 131904 (2005).
[23] K. Y. Zang, Y. D. Wang, S. J. Chua, L. S. Wang, and S. Tripathy, Appl. Phys. Lett. **88**, 141925 (2006).
[24] G. McHale, S. Aqil, N. J. Shirtcli, M. I. Newton, and H. Y. Erbil, Langmuir **21**, 11053 (2005).
[25] M. Reyssat, J. M. Yeomans, and D. Quèrè, EPL **81**, 26006 (2008).
[26] P. Tsai, R. G. H. Lammertink, M. Wessling, and D. Lohse, Phys. Rev. Lett. **104**, 116102 (2010).
[27] H. Kusumaatmaja, M. L. Blow, A. Dupuis, and J. M. Yeomans, EPL **81**, 36003 (2008).
[28] G. Wulff, Z. Kristallogr. **34**, 449 (1901).
[29] R. Kaischew, Comm. Bulg. Acad. Sci. (Phys.) **1**, 100 (1950).
[30] H. Kusumaatmaja and J. M. Yeomans, Langmuir **23**, 6019 (2007).